

BIOSTRATIGRAPHY AND PALEOENVIRONMENTAL ANALYSIS OF THE LOWER MIOCENE QOM FORMATION (JAAM AREA, CENTRAL IRANIAN BASIN)

BOTOND LÁZÁR^{1,6}, MOSTAFA FALAHATGAR², MEHDI SARFI², MĂDĂLINA-ELENA KALLANXHI³, RAMONA BĂLC^{4,5} & LÓRÁND SILYE^{1,6*}

¹Department of Geology, Babeş-Bolyai University, 1 Mihail Kogălniceanu Street, 400084, Cluj-Napoca, Romania.

²Damghan University, School of Earth Sciences, 36716-41167 Damghan, Iran.

³Albanian Geological Survey, Rr. Myslym Keta, Tiranë, Albania.

⁴Faculty of Environmental Science and Engineering, Babeş-Bolyai University, 30 Fântânele Street, 400084, Cluj-Napoca, Romania.

⁵Interdisciplinary Research Institute on Bio-Nano-Sciences, Babeş-Bolyai University, 42 Treboniu Laurian Street, 400271 Cluj-Napoca, Romania.

⁶Center for Integrated Geological Studies, Babeş-Bolyai University, 1 Mihail Kogălniceanu Street, 400084, Cluj-Napoca, Romania.

*Corresponding author. E-mail: lorand.silye@ubbcluj.ro

Associate Editor: Luca Giusberti.

To cite this article: Lázár B., Falahatgar M., Sarfi M., Kallanxhi M.-E., Bălc R. & Silye L. (2023) - Biostratigraphy and paleoenvironmental analysis of the Lower Miocene Qom Formation (Jaam area, Central Iranian Basin). *Riv. It. Paleontol. Strat.*, 129(3): 609-628.

Keywords: Benthic foraminifera; calcareous nannofossils; Burdigalian; paleoecology; paleogeography.

Abstract. Lower Miocene sediments from a previously not investigated outcrop of the Qom Formation (Central Iranian Basin) were studied for their foraminiferal and calcareous nannofossil content. The studied stratigraphic record is assigned to the upper part of calcareous nannofossil NN2 Zone/CN1c Subzone and to the benthic foraminiferal *Borelis melo melo* Zone of Burdigalian age. The diversity indices, benthic foraminiferal morphogroups, and quantitative investigation of assemblages (principal component and cluster analysis) suggest an overall shallow-marine depositional environment. This interpretation is well constrained based on the dominance of the B1 benthic foraminifera morphotype with biconvex, trochospiral calcareous test, and epifaunal habitat. The identified six cluster groups of benthic foraminiferal assemblages are confirmed by the principal component analysis too, and their distribution along the studied section argue for dynamic changes of the environment. This is well exemplified by a more or less constant shallowing, then deepening trend of the environment as revealed by the shifting from the high diversity, shallow-shelf assemblages of Cluster 5 and 6 toward the low diversity, near-shore *Ammonia tepida* and *Porosonion subgranosus* assemblage (Cluster 1), and back.

INTRODUCTION

In the earliest Miocene the Central Paratethys and the Mediterranean had a large-scale connection with the Indo-Pacific which facilitated the faunal exchange between the two oceanic realms (Rögl 1999). However, towards the end of Burdigalian

this connection was interrupted due to the collision between the African-Arabian and Iranian (Eurasian) plates. As a result, the marine faunal migration and exchange between the two marine provinces was interrupted (Harzhauser & Piller 2007; Rögl 1999). The timing of the final collision of the African-Arabian plates with the Iranian Plate (Coleman-Sadd 1982; Reuter et al. 2009; Rögl 1998b), hence the closure of the Tethyan seaway, is still under debate. The large benthic foraminiferal record suggests an

Received: September 8, 2022; accepted: September 11, 2023

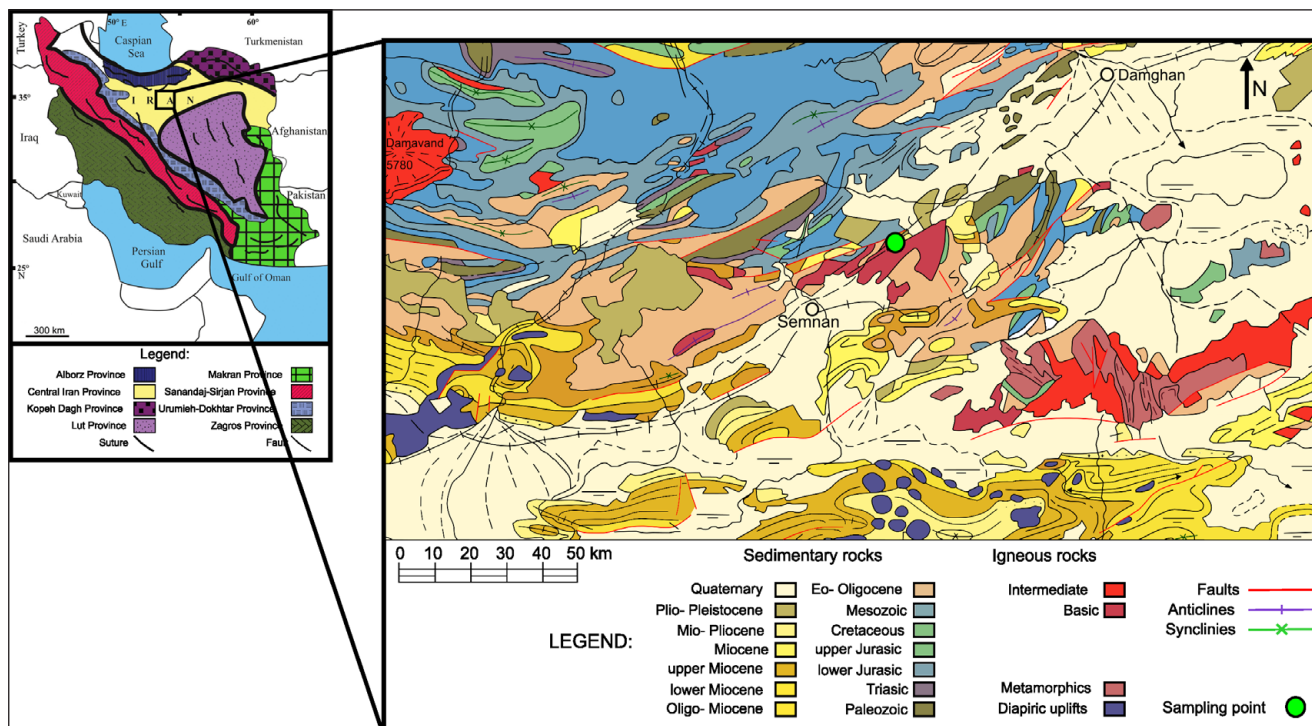


Fig. 1 - Geological map of the studied area. Redrawn and modified after the Geological Map of Iran (1: 2.500.000) compiled by the National Iranian Oil Company in 1957 and Heydari et al. (2003).

Aquitanian age (Adams et al. 1983), whilst the fossil mollusks and mammal record indicate a Burdigalian age (Robba 1986; Rögl & Steininger 1983; Whybrow 1984) for this event. The collision between the two plates led to the formation of a volcanic arc, thus, the Qom Basin become a back-arc basin in the Miocene (Reuter et al. 2009; Schuster & Wielandt 1999; Seddighi et al. 2012).

These significant paleobiogeographic and palaeoceanographic changes (Reuter et al. 2009) coincided with the deposition of the Lower Miocene Qom Formation in the Central Iranian Basin, hence this lithostratigraphic unit offers insights into the evolution and isolation of the Paratethys. However, the age of the Qom Formation it is still not well constrained, although it is in the focus of various studies since Loftus (1855). The results so far evidenced that the age of this lithostratigraphic unit spans between Oligocene to Miocene based on the smaller and larger benthic, and planktonic foraminiferal record of the Qom Formation (Behforouzi & Safari 2011; Daneshian & Dana 2007; Mohammadi & Ameri 2015; Nouradini et al. 2015; Rahaghi 1976, 1980; Yazdi-Moghadam et al. 2021). However, the age of the different parts of the Qom Formation, which covers more than 1800 km in three basins (Mohammadi 2022), is far from being well constrained.

Furthermore, a proper paleoenvironmental interpretation of this stratigraphic unit is essential for exploration, because the bioclastic limestones host hydrocarbon reserves with major economic interest (Reuter et al. 2009).

In order to better constrain the depositional environment of the Qom Formation, the aims of this study are: 1. a first detailed calcareous nannofossils investigation to better constrain the depositional time-interval of the Qom Formation; 2. the use of foraminiferal and calcareous nannofossil biostratigraphy based on assemblages' comparison, and correlation to various standard zonation; and 3. depositional history and paleoenvironmental reconstruction of the Early Miocene interval of the Qom Formation in the Central Iranian Basin.

GEOLOGICAL SETTING

The Central Iran Basin belongs to and is classified as one of the structural tectonic zones of the Iranian territory (Stöcklin & Setudehina 1991) exhibiting complex geological units (Fig. 1) spanning from Paleozoic to Recent (Letouzey & Rudkiewicz 2005; Yazdi-Moghadam et al. 2018). In the south, the basin is separated from the Zagros Mountains

by the remnants of the Neo-Tethys. The closure of the Neo-Tethys occurred in the Late Cretaceous, while the Arabian Plate continued its movement toward the Iranian Plate (Eurasia) until the collision of the two plates around the Oligocene-Miocene boundary (Yazdi-Moghadam et al. 2021).

The sedimentary record of the Qom Formation was deposited in the Tethyan Seaway in Central Iran (Qom back-arc basin), as well as in the Sanandaj-Sirjan strip (fore-arc basin) and Urmia-Dokhtar magmatic arc zone (inter-arc basin), therefore covering a large area (Berberian 1983; Daneshian & Dana 2019; Mohammadi et al. 2013; Reuter et al. 2009). Stratigraphically it is positioned between two continental formations (the Lower Red and the Upper Red formations) and consists of alternating marls, limestones, and shelly limestones (Seyrafian & Toraby 2005; Stöcklin & Setudehina 1991). The lithological complexity of the Qom Formation was already documented by the first geological studies targeting this formation and done by Loftus (1855), Tietze (1875), Kühn (1933), Gansser (1955), Abaie et al. (1964), and Bozorgnia (1966). More detailed work was done by Furrer & Soder (1955) who subdivided the Oligocene and Miocene Qom Formation in the type locality into six members (a, b, c, d, e, f), whilst Soder (1959) further extended the C unit into 4 subunits (c-1, c-2, c-3 and c-4) and Bozorgnia (1966) recognized up to ten members within the Qom Formation. More recently, Stöcklin (1991) combined the previous subdivisions of the Qom Formation, hence finally subdividing it into 9 members.

Previous biostratigraphy and paleoenvironmental studies of the Qom Formation were mainly based on the data provided by larger benthic foraminifera (LBF), smaller benthic foraminifera, planktonic foraminifera, corals, bryozoans, and ostracods. Rahaghi (1976, 1980) described LBF assemblages which later were further detailed by Daneshian & Chegini (2007), who conducted studies on benthic foraminiferal assemblages of the Qom Formation exposed in the area of Semnan, and by Behforouzi (2011) who focused on the biostratigraphy and paleoecology of the assemblages in the Chenar area. Rezaeian (2008) concluded that the Qom Formation was deposited on the southern margin of the Alborz Mountains. Behforouzi (2011) used thin sections in order to address the foraminiferal biostratigraphy and paleoecology of the

Qom Formation in Chenar area (NW Kashan, central Iran), whilst Karevan et al. (2014) studied the biostratigraphy and paleoecology of scleractinian corals in order to reconstruct the depositional environment of the Qom Formation in NE Dalijan, Central Iran. The LBF assemblages from the Central Iranian Basin were first described by Mohammadi & Ameri (2015). Nouradini et al. (2015) focused on foraminiferal paleoecology in order to refine the paleoenvironmental reconstruction of the Qom Formation in NE Isfahan, Central Iran. A relatively diverse (15 genera and 28 species) planktonic foraminiferal assemblage was recovered by Daneshian & Ghanbari (2017) from the Qom Formation in the Zanjan area (NW Iran). Daneshian & Dana (2019) studied the Lower Miocene benthic foraminiferal assemblages from Central Iran and recognized pelagic facies. Recently, Yazdi-Moghadam et al. (2021) investigated the Lower Miocene benthic foraminiferal and coralline algal assemblages from the Qom Formation in the northwestern region of Iran.

The investigated area is located 21 km west of the Jaam village (east of Semnan) in the northernmost part of the Central Iran Basin. It is separated from the Alborz Mountains to the north by the Attari fault (Alavi-Naini 1997), a 25 km long fault located beneath the Jaam area. Here the Cenozoic starts with Eocene marls (Dozahir Marls) and continue with shallow marine lower Oligocene and middle Oligocene deposits (marls, gypsum, sandstone and conglomerates). The upper Oligocene sequence is represented by the Lower Red Formation (intercalations of sandstone, reddish conglomerate and marls), and continues upward with lower Miocene marine transgressive succession (Qom Formation). The Miocene deposits are overlain by the Miocene/Pliocene terrigenous rocks belonging to the Upper Red Formation (sandstone, red conglomerates, red marls and siltstones). The youngest deposits in the Jaam area are Pliocene-Pleistocene conglomerates. In some parts of the Jaam area however, the volcanic rocks overlie unconformably the Qom Formation (Alavi-Naini 1997).

MATERIAL AND METHODS

The Jaam section (N: 35°43'34", E: 53°38'43") is located in the proximity of Semnan city, about 180 km east of Tehran (Fig. 1). The strati-

Series/ Subseries	Stage	Biozones
Lower Miocene	Burdigalian	<i>Borelis melo melo</i> - <i>Borelis melo crudica</i>
	Aquitanian	<i>Miogypsina</i> - <i>Elphidium</i> sp. - <i>Peneroplis farsensis</i> Indeterminated zone
Oligocene	Chattian	<i>Archaias asmaricus/ hensoni</i> - <i>Miogypsina complanatus</i>
	Rupelian - Chattian	<i>Lepidocyclina</i> - <i>Operculina</i> - <i>Ditrupe</i>
	Rupelian	<i>Nummulites vascus</i> - <i>Nummulites fichtelli</i>
Eocene - Oligocene		<i>Globigerina</i> spp. - <i>Turborotalia cerrazoulensis</i> - <i>Hantkenia</i>

Fig. 2 - The foraminiferal biozonation of the Qom Formation (based on Laursen et al. 2009 and van Buchem et al. 2010).

graphic thickness of the Qom Formation in this area is around 450 m, and the sediments consist mainly of marls, and marlstone presenting different stages of cementations, with their color varying between green, brown, grey, or light grey. However, limestones are often interlayering between the marls or marlstones. Samples (~ 100-200 g each) were collected from the marly intervals, and special attention was paid on those intervals where lithological changes were observable.

Foraminiferal assemblages

Thirty-eight samples were collected and analyzed for foraminifera. The samples were prepared using the standard micropaleontological technique, with some minor modifications. Since the samples were fairly well cemented and the microfossils presented a poor to moderate preservation, we oven-dried (at 50°C) and weighed the materials, then treated them with a 3% hydrogen peroxide solution for 12 hours. The disintegrated samples were washed over a 63 µm mesh using tap water. The residues were dried overnight in the oven at 50°C. If needed, the above-mentioned steps were repeated. The dried residue was dry sieved over a >125 µm mesh and split with an ASC microsplits until an aliquot of ~250-300 specimens of benthic foraminifera was obtained. The entire benthic foraminiferal content (>125 µm) of the selected split was picked under an Optika stereomicroscope. The specimens were sorted and counted, and the resulted data was used for proxy and statistical calculations. The identification at species level of the collected specimens was done using a ZEISS Stemi 508 stereomicroscope with 125X and a Hitachi SV8230 SEM machine.

The standard biozonations used in the present study follow the concepts of Laursen et al. (2009) and van Buchem et al. (2010) (Fig. 2). Their biozo-

nation is based on the Asmari Formation, which is the lithostratigraphic equivalent of the Qom Formation (Abbassi et al. 2016).

The diversity indices i.e., total number of taxa (taxa), the dominance (D) of the identified species estimated using the Simpson diversity index, the Shannon-Wiener and Fisher's α were calculated using Past 4.07b (Hammer & Harper 2006; Hammer et al. 2001). We used the Shannon-Wiener index because it estimates the diversity of the species based on their relative abundance and richness (Spellerberg & Fedor 2003), and the Fisher's alpha index as it is used to differentiate between the samples varying in the number of specimens (Fisher et al. 1943; Hammer & Harper 2006). The abundance of the benthic foraminifera in a sample was calculated by dividing the number of recovered foraminiferal specimens with the multiple of the dried weight of the samples and the used split fraction.

PLATE 1

Lower Miocene benthic foraminiferal microphotographs (SEM).

Scale bar 100 µm.

- 1 - *Oligita pacifica* (Cushman, 1924).
- 2 - *Textularia* sp. 1 (Defrance, 1824).
- 3 - *Textularia sagittula* (Defrance, 1824).
- 4 - *Spiroplectinella* sp. (Kisel'sman, 1972).
- 5 - *Bulimina* aff. *elongata* (d'Orbigny, 1826).
- 6 - *Triloculina* sp. 2 (d'Orbigny, 1826).
- 7 - *Triloculina* sp. 1 (d'Orbigny, 1826).
- 8 - *Cycloforina* cf. *gracilis* (Karrer, 1867).
- 9 - *Ammonia beccarii* (Linnaeus, 1758).
- 10 - *Elphidium crispum* (Linnaeus, 1758).
- 11 - *Elphidium* sp. (Montfort, 1808).
- 12 - *Porosonion subgranosus* (Egger, 1857).
- 13 - *Pararotalia* aff. *aculeata* (d'Orbigny, 1846).
- 14 - *Borelis melo* (Fichtel & Moll, 1798).
- 15 - *Rosalina* aff. *obtusa* (d'Orbigny, 1846).
- 16 - *Nonion commune* (d'Orbigny, 1846).
- 17 - *Articulina* sp. 1. (d'Orbigny, 1826).

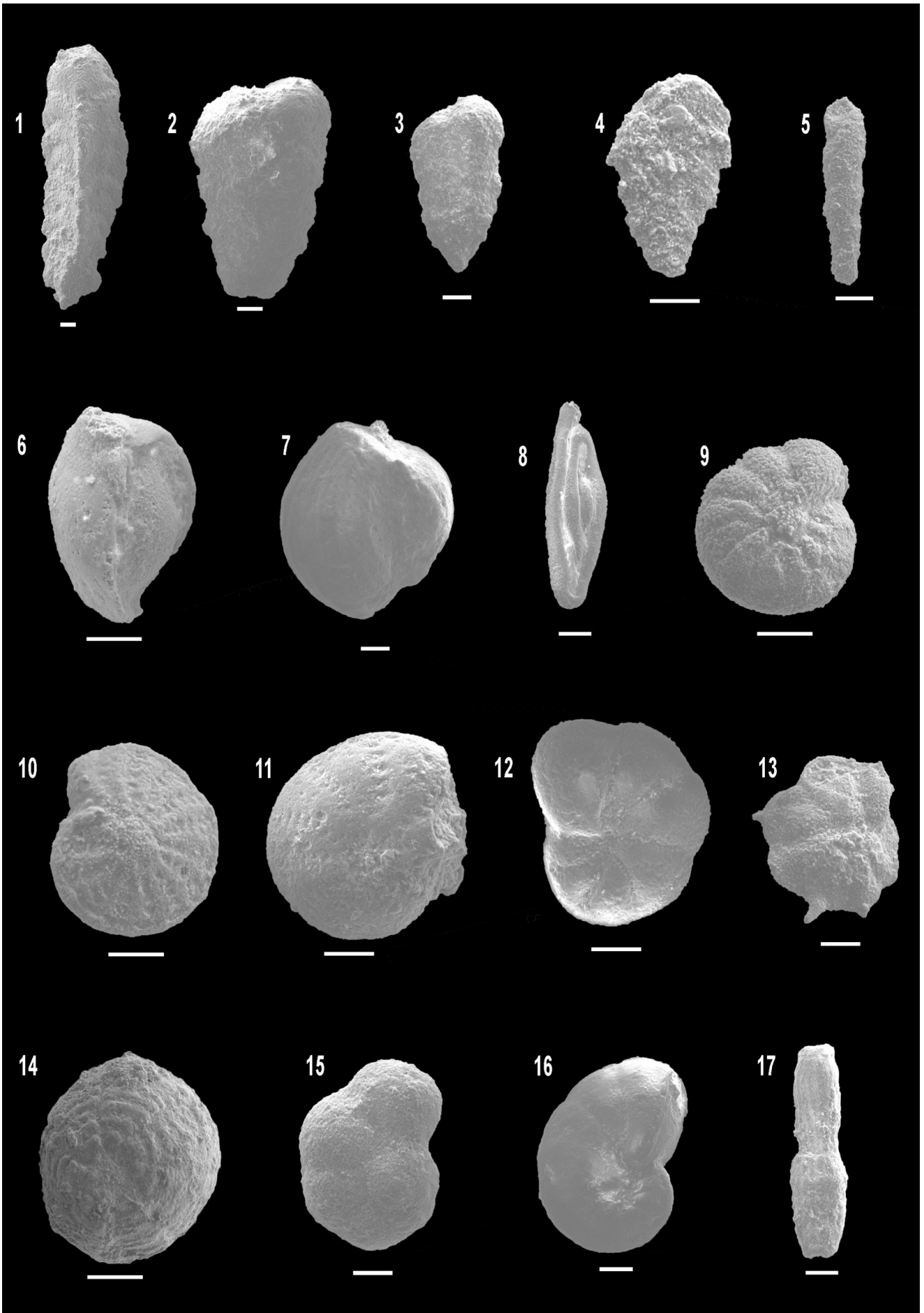


PLATE 1

The statistical analysis was done using Past 4.07b (Hammer & Harper 2006; Hammer et al. 2001). The hierarchical cluster analysis (Q-mode) is based on Ward's method, and Euclidean similarity index without stratigraphic constraint. The PCA (Principal Components Analysis) was performed using variance-covariance matrix. The analyzed dataset included only those benthic foraminiferal taxa which had at least $\geq 1\%$ relative abundance in at least 1 sample. The barren samples were also excluded from the statistical treatment analysis.

In this study, we analyzed the foraminiferal assemblages morphotypes based on Chan et al. (2017). Four morphogroups were determined (A, B, C, and D), and these were further subdivided into different morphotypes based on their test shape. Since the analysis was designed for benthic foraminifera, we ignored the planktonic species. Furthermore, we excluded the unidentified benthic foraminiferal species. The decisive factors for the morphogroups and morphotypes are based on their shell morphology, life position, and mode of life.

Calcareous nannofossils

Seventy samples were investigated for calcareous nannofossils' content, from which 62 samples contained moderately to poorly preserved calcareous nannofossils, while eight samples were barren. The smear slides were prepared according to the standard techniques (Bown & Young 1998) and were examined under polarized light in cross-nichols (XPL) and bright field (BF) with a Zeiss light microscope (LM) at 1000x magnification.

The species belonging to *Reticulofenestra*, which are among the most common in the investigated material, were separated using a size-based identification combined with some morphological characteristics (see Nannotax3 Young et al. 2022; Kallanxhi 2023): *Reticulofenestra minuta* (very small placoliths $< 3 \mu\text{m}$), *R. antarctica* (small placoliths with a size of $3\text{--}5 \mu\text{m}$ and closed central area; sensu Wade & Bown 2006), *R. haqii* (small placoliths with size $3\text{--}5 \mu\text{m}$ and a central opening), *R. gelida* (medium to large specimens, $> 5\text{--}10 \mu\text{m}$; with a nearly closed central area by a pore/long pore/slit); *R. daviesii* (medium sized placoliths, size $5\text{--}8 \mu\text{m}$ and central-area surrounded by a ring of pores) and *R. pseudumbilicus* (medium to large sized placoliths, $> 5 \mu\text{m}$, elliptical with central opening). The specimens of *R. pseudumbilicus* were separated into two size classes: $> 5\text{--}7 \mu\text{m}$, and > 7

μm , the last one being dominant.

The calcareous nannofossil relative abundance per sample was assessed semi-quantitatively at first look, as follows: F – Few (1 specimen/FOV), R – Rare (1 specimen/2-10 FOVs), VR – Very rare (1 specimen/11-100 FOVs), VVR – Very very rare (1 specimen/ $>100\text{--}300$ FOVs), XR – Extremely rare (1 specimen/sample) and B – barren. The calcareous nannofossil assemblage was separated into autochthonous and reworked. The biostratigraphy follows mainly the concepts of Martini (1971), and Okada and Bukry (1980). Abbreviations in the text mean as follows: FO - First Occurrence and LO – Last Occurrence.

RESULTS

Benthic foraminiferal assemblages

More than 10.000 benthic foraminifera specimens were picked and identified from the investigated samples, resulting in the identification of 41 different taxa (Fig. 3; Plate 1; Appendix 1, Table 2). The average taxa number per sample is 15. The assemblages with the highest taxa number (20) were recovered either from the bottom (EQ - 09) or from the upper part (EQ - 51 and EQ - 64) of the studied section. The lowest taxa number (9) was recorded in the middle part of the studied stratigraphic record (EQ - 36). Changes can be observed in the number of the identified taxa: a notable increase from 9 (EQ - 36) to 20 (EQ - 51), or a drop from 19 (EQ - 69) to 14 (EQ - 71). In some cases, however, the transition between two neighboring samples shows only a minor change in the number of taxa e.g., samples EQ - 78 and EQ - 81.

The most common species found throughout the section are *Ammonia beccarii*, *Ammonia tepida*, *Porosonion subgranosus*, and species belonging to the *Elphidium* and *Triloculina*, but the continuous presence in low abundance of *Borelis melo* marker taxa was also observed. An interesting finding was the occurrence of *Oligita pacifica* since it is for the first time reported from this area. Furthermore, it is important to note the almost complete absence of the planktonic foraminiferal species from the studied samples.

Diversity indices

The taxa count resulted from the analysis of the benthic foraminiferal assemblages were used to

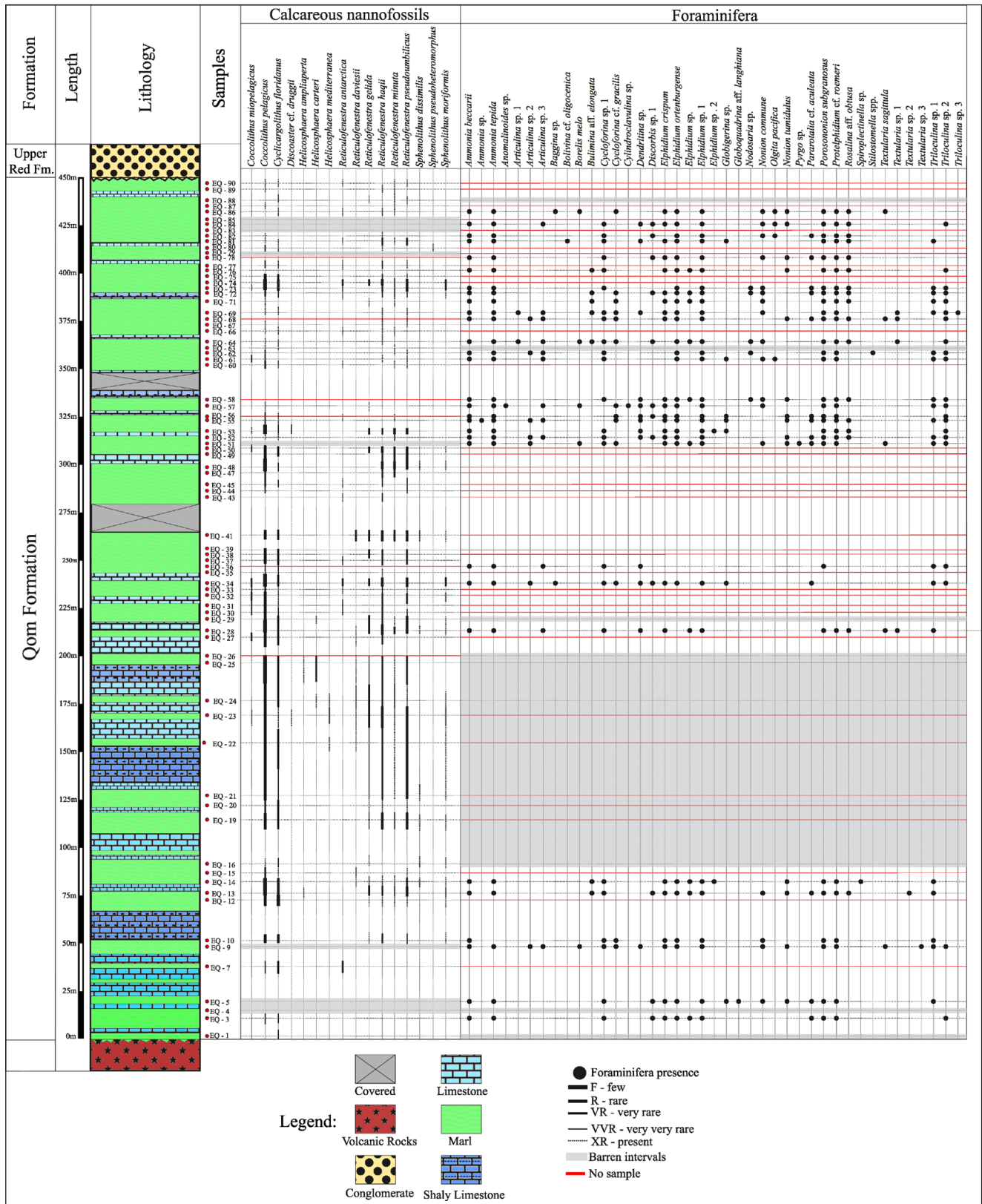


Fig. 3 - Lithology and the distribution of the calcareous nannofossil and foraminiferal taxa along the studied section.

calculate the abundance, dominance, taxon numbers, Shannon-Wiener, and Fisher's alpha indices (Fig. 4).

The abundance of the benthic foraminiferal assemblages in the studied samples is moderate. Its values range from ~ 4 to 714 specimen/g dry sedi-

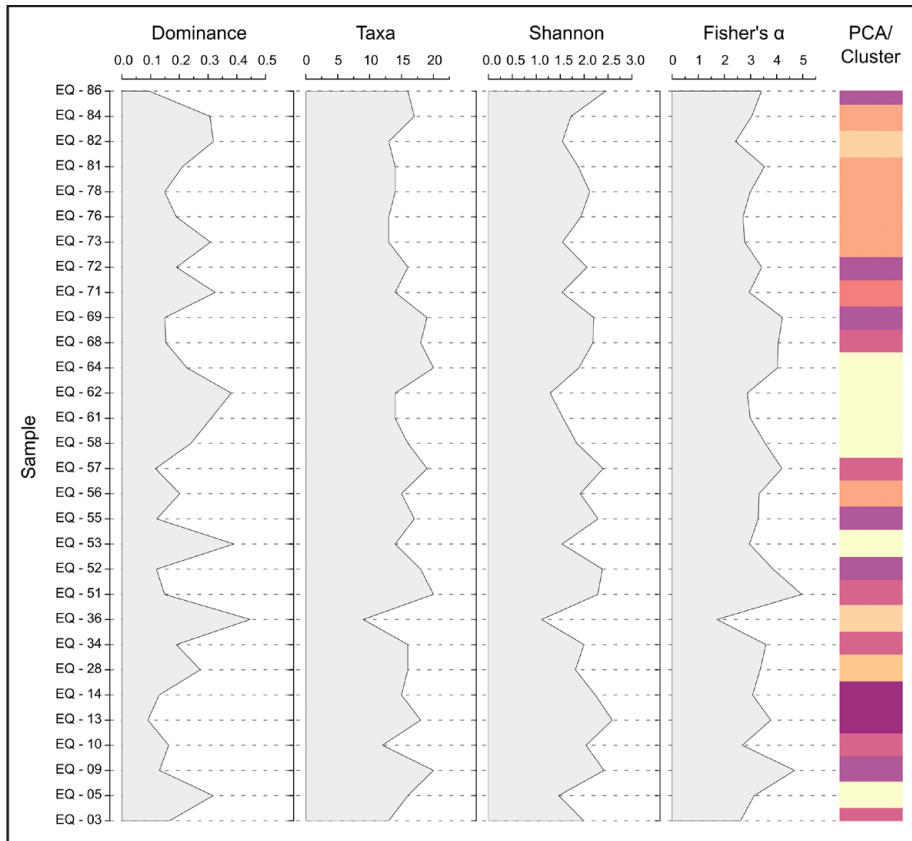


Fig. 4 - The diversity indices of the benthic foraminiferal assemblages along the section. The colors correspond with the cluster and PCA analysis (see fig. 6).

ment. The lowest value is registered in sample EQ-81 (with *Elphidium* sp. 1 as dominant taxon), while the highest can be found in the EQ-82 (with *Ammonia beccarii* as dominant taxon). The average abundance of the benthic foraminifera in the samples is ~ 225 specimens/g dry sediment.

None of the investigated assemblages can be characterized by a clear, pronounced dominance of any taxon. Even the value of 0.5 of the dominance was not reached by any of the assemblages. The highest D is registered in the lower part of the section (EQ-36, D = ~0.45). The assemblages with the

lowest D values (~ 0.10) were recovered from the bottom part (EQ - 13) or the upper part of the (EQ - 86) studied sedimentary record. The average number of the dominance is low (~0.20).

The Fisher's alpha diversity index has values between 1.72 - 4.96. The lowest value is registered in the sample EQ-36, while the peak is found in the EQ-51. In case of the samples EQ-69, EQ-68, and EQ-64 the Fisher's values are almost identical (4-4.2). The Shannon-Wiener diversity index registers a range from around 1(EQ-36) to 2.5 (EQ-13). The values of this diversity index fluctuate throughout

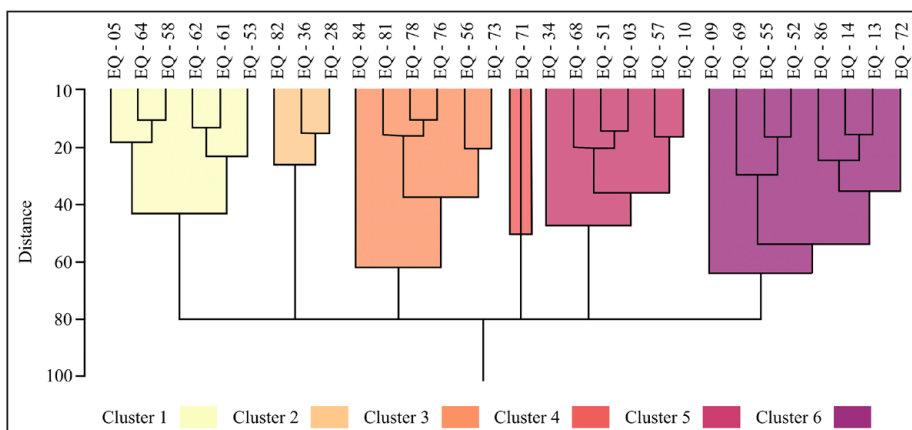


Fig. 5 - Grouping of the samples by multivariate clustering analysis (Ward's method) performed on the benthic foraminiferal assemblages.

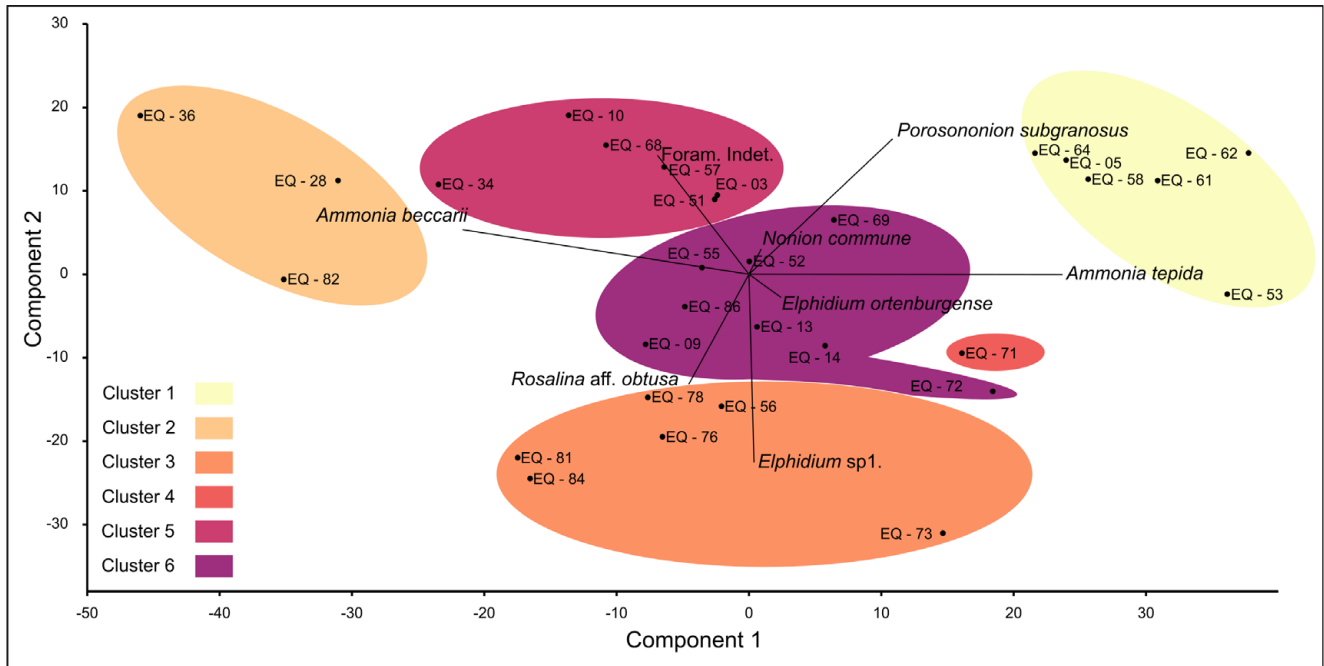


Fig. 6 - First two components of the principal component analysis carried out on the smaller benthic foraminiferal dataset. The graph also shows the grouping of the samples according to the cluster analysis.

the studied section. Furthermore, the Fisher's alpha and the Shannon-Wiener indexes have very similar trends.

Cluster analysis

The hierarchical clustering resulted six well constrained clusters (Fig. 5).

Cluster 1 – groups six samples (EQ-05, EQ-64, EQ-58, EQ-61, EQ-62, and EQ-53) characterized by a high relative abundance of *Ammonia tepida* and *Porosonion subgranosus*. The first one's relative abundance in a given sample can be as high as 60%, while the last peaks at around 45%. Besides the dominant species, the presence of some benthic foraminifera taxa (*Elphidium ortenburgense*, *Protelphidium* cf. *roemeri*, and *Cycloforina* cf. *gracilis*) with low relative abundance could be observed.

Cluster 2 – includes only three samples (EQ-28, EQ-36, and EQ-82) with high relative abundance (48-61%) of *Ammonia beccarii*. In addition to *A. beccarii*, *C. cf. gracilis*, and *P. subgranosus* are present in low relative abundance (4.6-6.7%).

Cluster 3 – groups six samples (EQ-84, EQ-81, EQ-78, EQ-76, EQ-56, and EQ-73) having in common high relative abundance of *Elphidium* sp. 1 (7.8-36.8%) and *Rosalina* aff. *obtusata* (0-52.2%). These species are accompanied by taxa having rather similar relative proportion: *A. tepida*, *A. beccarii* (1.4-

30.8%), *E. ortenburgense* (1-10.2%), *P. cf. roemeri* (0.4-7%) and *P. subgranosus* (1.1-13-7%).

Cluster 4 – consists of one sample (EQ-71) with a high relative abundance of *Bulimina* aff. *elongata* (~50%). In this sample *A. tepida* makes up almost 30% of the identified benthic foraminifera. Apart from these two taxa, the relative abundance of various *Elphidium* and *Triloculina* species is notable.

Cluster 5 – groups six samples (EQ-34, EQ-68, EQ-51, EQ-03, EQ-57, EQ-10) with common *A. beccarii* (8.6-19.3%). Other abundant species in the samples of this cluster are *Nonion commune*, *E. ortenburgense*, *P. subgranosus* and taxa of the genera *Triloculina*, and *Cycloforina*.

Cluster 6 – groups together 8 samples (EQ-09, EQ-69, EQ-55, EQ-52, EQ-86, EQ-14, EQ-13, EQ-72) characterized by the quite equal relative abundance of *A. beccarii*, *A. tepida*, *Elphidium*, *Cycloforina*, and *Triloculina*.

Principal Component Analysis

The PCA analysis (Fig. 6.) was performed to gain complementary data on the separation of the benthic foraminiferal assemblages into different groups. The first two principal components (PC 1 and 2) can explain 52.47% of the variance present in the data.

PC 1 explains 35.35% of the variance and separates the samples with a clear dominance of *Ammonia tepida*, *Nonion commune*, and *Porosonion subgranosus* from the samples with a relatively high abundance of *Ammonia beccarii*, *Triloculina* sp. 2, *Bulimina* aff. *elongata* and *Rosalina* aff. *obtusa*.

PC 2 can explain around 16.9% of the variance. Its separation of the samples is based on the differences in the relative abundance of *A. beccarii*, *N. commune*, *P. subgranosus*, and *Cycloforina* cf. *gracilis* from the samples dominated by *Elphidium* sp. 1, *R. aff. obtusa*, *B. aff. elongata*, and *Triloculina* sp. 1.

The PCA analysis suggests that sample EQ-72 grouped in Cluster 6 is an outlier. The difference between the sample EQ-72 and the rest of the samples belonging to Cluster 6 is linked to the significant difference as regards the relative abundance of *A. tepida* in EQ-72 (36.6%) versus the rest of the samples of Cluster 6 (2.4%–18.8%). Since the separation of the samples by PC 1 is mainly based on the relative abundance of *A. tepida*, sample EQ-72 was moved on the horizontal axis from the rest of the samples belonging to Cluster 6. Thus, explaining its somewhat strange position on the PCA graph.

Morphogroups

Morphotype analyses were carried out on the benthic foraminiferal assemblages (Fig. 7). The definition of morphotypes is mainly based on the life position and shell morphology with references to extant species (Chan et al. 2017), and our analysis is focused on the most important morphotypes present in the samples.

The most abundant species belong to the B1 morphotype, which is dominant almost throughout all the studied samples (Fig. 8). The taxa of this morphotype have biconvex shell with trochospiral growth, and prefer an epifaunal habitat. The main benthic foraminifera species of this group are *Ammonia beccarii* and *A. tepida*. These species are known for surviving extreme environmental conditions and stress factors living in a shelf environment (Murray 2006), and are able to adapt to and survive at low oxygen concentrations (Kitazato & Tsuchiya 1999; Moodley & Hess 1992). They are also often found in a shallow-water marine, estuary systems (Mendes et al. 2004; Morigi et al. 2005; Polovodova et al. 2009).

The morphotype A1 has a variable proportion along the studied section, but it is more common in the lowermost and upper middle part of it. Oppor-










Morphogroups	Morphotypes	Test form	Main genera
A	A1 	Biconvex Planspiral	<i>Elphidium</i>
	A2 	Flattened-depressed Planspiral	<i>Peneroplis</i> <i>Operculina</i>
B	B1 	Biconvex Trochospiral	<i>Rotalia</i> <i>Ammonia</i>
	B2 	Planconvex Trochospiral	<i>Discorbinella</i>
C	C1 	Miliolid- Triloculina	<i>Triloculina</i>
	C2 	Miliolid- Pyrgo	<i>Pyrgo</i>
	C3 	Miliolid- Spherical	<i>Borelis</i>
D	D1 	Cylindrical Uniserial	<i>Stilostomella</i> <i>Nodosariid</i>
	D2 	Agglutinated Biserial	<i>Textularia</i>

Fig. 7 - Foraminiferal morphotypes based on shell morphology and their living habitat. Redrawn and modified after Chan et al. (2017).

tunistic feeding is characteristic for the benthic foraminiferal species placed in this group (species belonging to the *Elphidium* genus). Species belonging to the genus *Elphidium* are considered to live in a shallow-water marine environment (Frezza & Carboni 2009; Levy et al. 1995; Murray 1991). The species of this morphotype prefer somewhat similar conditions (i.e. shallow marine environment) as the *Ammonia* (Murray 2006), but are more sensitive to the salinity changes. Several species of this morphotype (e.g., *Elphidium crispum*) are bloom feeders: they rapidly grow and reproduce during phytoplankton bloom periods, thus causing patchiness in their appearance (Murray 1991).

The C1 morphotype groups species belonging to the *Triloculina*. They are known to survive in hypersaline conditions (up to 65 ppt), hence, an increase in the salinity levels can explain the sporadic accentuated presence (Murray 1991).

The D1 morphotype is almost non-present except in sample EQ-71. The marked increase of the percentage of this morphotype is caused by a high relative proportion of *Bulimina* aff. *elongata* in

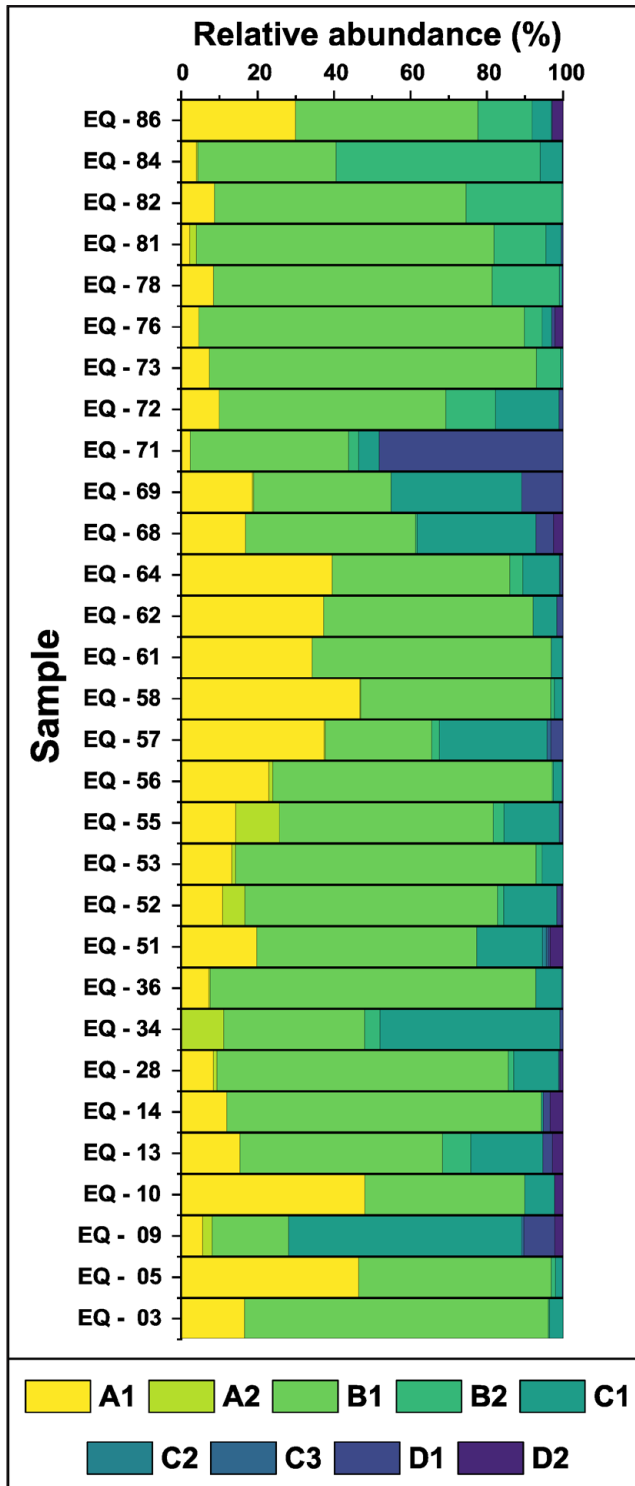


Fig. 8 - Relative abundance (%) of the benthic foraminiferal morphotypes in the studied samples.

sample EQ-71. *Bulimina*, a common shelf genus is known to survive in low-oxygen environments (Colliss & Emerson 1990; Murray 2006). Also, they live in shallow waters with a relatively high organic carbon content (Hermelin & Shimmield 1990; Miller & Lohmann 1982).

Morphotype B2 has an increased relative abundance in the upper part of the studied section, due to the presence of *Rosalina* aff. *obtusa*. The common normal marine shelf taxa belonging to the *Rosalina* genus can produce an organic glue in order to attach themselves to plants thus surviving even in high energy zones (Langer 1993).

The A2 morphotype (*Dendritina*) is known to live in a shallow, tropical environment up to 20 m water-depth (Betzler & Scmitz 1997). They can dwell in a high or a low energy zone without discrimination (hard or seagrass bed) to their substrate (Leutenegger 1984; Reiss & Hottinger 1984).

The C2 morphotype consist of the species belonging to the genus *Pyrgo*. Based on Murray (1991) they prefer normal salinity (~35‰) and are almost completely missing in hypersaline conditions.

The C3 is represented by *B. melo* which indicates a warm (25°C), shallow-water marine habitat (El Baz et al. 2018; Murray 1991). Their living depth and distribution is chiefly dependent upon the symbiont they host in their shell (Leutenegger 1984).

The species belonging to the *Textularia* genus are placed into the D1 morphotype. These species thrive in environments influenced by open marine systems and does not prefer the muddy sediments (Haunold 1999).

Calcareous nannofossil assemblage composition and diversity

The calcareous nannofossils assemblage (Appendix 2; Plate 2) contains a total of 83 taxa, from which 31 species were considered in situ and comprise typical Lower Miocene species, while 52 species are reworked from Mesozoic and Paleogene. The long ranging taxa like *Braarudosphaera bigelowii*, *Coccolithus pelagicus*, *Cyclicargolithus floridanus*, *Reticulofenestra minuta* and *Sphenolithus moriformis* were considered part of the autochthonous assemblage. The dominating calcareous nannofossil families are as follows: Helicosphaeraceae (with nine species), Noelaerhabdaceae (with seven species), Sphenolithaceae (with four species), Coccolithaceae and Discoasteraceae (with four species each). The rest of the remaining families are represented by only one species each (Braarudosphaeraceae, Calcidiscaceae and Pontosphaeraceae). The in-situ taxa (*C. pelagicus*, *C. floridanus*, *Reticulofenestra haqii*, *R. minuta* and *Reticulofenestra pseudoumbilicus*) belong to the most common species found and have a continuous presence along the studied sedimenta-

ry record (Fig. 3). Less abundant and with discontinuous distribution along the section are: *Coccolithus miopelagicus*, *Reticulofenestra antarctica*, *Reticulofenestra daviesii*, *Reticulofenestra gelida* and *Sphenolithus moriformis*. Most of the identified species i.e., *B. bigelowii*, *Clauisococcus subdistichus*, *Coronocyclus nitescens latus*, *Discoaster adamanteus*, *Discoaster deflandrei*, *Discoaster* cf. *druggii*, *Discoaster* sp., *Helicosphaera ampliapertura*, *Helicosphaera carteri*, *Helicosphaera euphratis*, *Helicosphaera mediterranea*, *Helicosphaera minuta*, *Helicosphaera vedderi*, *Helicosphaera* cf. *watkinsii*, *Helicosphaera* sp. 1, *Helicosphaera* sp., *Pontosphaera multipora*, *Sphenolithus conicus*, *Sphenolithus dissimilis*, *Sphenolithus pseudoheteromorphus*, *Sphenolithus* sp. and *Umbilicosphaera rotula* are scarce and very rare to extremely rare.

Helicosphaera sp. 1 is a large helicolith with flat appearance (length is 9 μm and width is 6 μm), elliptical outline and crenulated margins, with no visible flange and no developed wing, only a very small spur being present. The general appearance of this species under XPL (90°) is bright when oriented parallel with one of the axes, while when inclined at approximately 30-45°, the central area becomes shadowed, displaying pseudo-extinction lines formed by a thin line along the length of the helicolith, and two thicker lines parallel to the short axis, which occupy the centre. The centre appears to be closed, the only perforations present are only two small pores which are visible in both XPL and BF and encase the central area.

DISCUSSION

Age assignment

The presence of the *B. melo* throughout the studied stratigraphic record support the assignment of the investigated foraminiferal assemblages to the *Borelis melo melo* Biozone (Laursen 2009; van Buchem et al. 2010; Sakhavati et al. 2020), and suggest a Burdigalian age (Early Miocene) for the Qom Formation at the studied site. This interpretation agrees with the age assignment of other *B. melo* bearing Lower Miocene deposits of Iran and Saudi Arabia (Chan et al. 2017; Daneshian & Dana 2007; Heidari et al. 2014; Hughes 2014; Vaziri-Moghaddam 2010; Sakhavati et al. 2020). Furthermore, the Burdigalian age is confirmed based on the known paleogeography: the migration of the genus *Olgita* into the study area from its nearest

reported occurrence in the Persian Gulf (Al-Enezi et al. 2020) was only possible until the formation of the so called *Gomphotherium* Landbridge in the late Burdigalian (Rögl 1998a).

PLATE 2

Lower Miocene calcareous nannofossils microphotographs. The images were captured in crossed polarized light (XPL) and in bright field (BF). The scale bar is of 2 μm (pictures 1-22) and 5 μm (pictures 23-24).

- 1 - *Coccolithus miopelagicus* Bukry, 1971 (sample EQ23, XPL).
- 2 - *Coccolithus pelagicus* (Wallich, 1877) Schiller, 1930 (sample EQ73, XPL).
- 3 - *Cyclicargolithus floridanus* (Roth & Hay, in Hay et al., 1967) Bukry, 1971 (sample EQ23, XPL).
- 4 - *Reticulofenestra pseudoumbilicus* (Gartner, 1967) Gartner, 1969 (sample EQ14, XPL).
- 5 - *Reticulofenestra baqii* Backman, 1978 (sample EQ41, XPL).
- 6 - *Reticulofenestra minuta* Roth, 1970 (sample EQ14, XPL).
- 7 - *Reticulofenestra daviesii* (Haq, 1968) Haq, 1971 (sample EQ14, XPL).
- 8 - *Umbilicosphaera rotula* (Kamptner, 1956) Varol, 1982 (sample EQ29, XPL).
- 9 - *Helicosphaera ampliapertura* Bramlette & Wilcoxon, 1967 (sample EQ13, XPL).
- 10 - *Helicosphaera ampliapertura* Bramlette & Wilcoxon, 1967 (sample EQ25, XPL).
- 11 - *Helicosphaera mediterranea* Müller, 1981 (sample EQ23, XPL).
- 12 - *Helicosphaera carteri* (Wallich 1877) Kamptner, 1954 (sample EQ25, XPL).
- 13 - *Helicosphaera* cf. *watkinsii* da Gama & Varol, 2013 (sample EQ19, XPL).
- 14 - *Helicosphaera minuta* Müller, 1981 (sample EQ50, XPL).
- 15-17 - *Helicosphaera* sp. 1 Kamptner, 1954 (sample EQ24, fig. 15 - 90° XPL, fig. 16 - 90° BF and fig. 17 - 30° XPL).
- 18 - *Sphenolithus dissimilis* Bukry & Percival, 1971 (sample EQ19, XPL).
- 19-20 - *Sphenolithus pseudoheteromorphus* Fornaciari & Agnini, 2009 (sample EQ15, XPL, two orientations; fig. 19 at 0° and fig. 20 at 45°).
- 21 - *Sphenolithus pseudoheteromorphus dissimilis* Bukry & Percival, 1971 (sample EQ14, at 45° XPL).
- 22 - *Discoaster* cf. *druggii* Bramlette & Wilcoxon, 1967 (sample EQ23, BF).
- 23 - *Discoaster* cf. *druggii* Bramlette & Wilcoxon, 1967 (sample EQ53, BF).
- 24 - *Discoaster* cf. *druggii* Bramlette & Wilcoxon, 1967 (sample EQ53, BF).

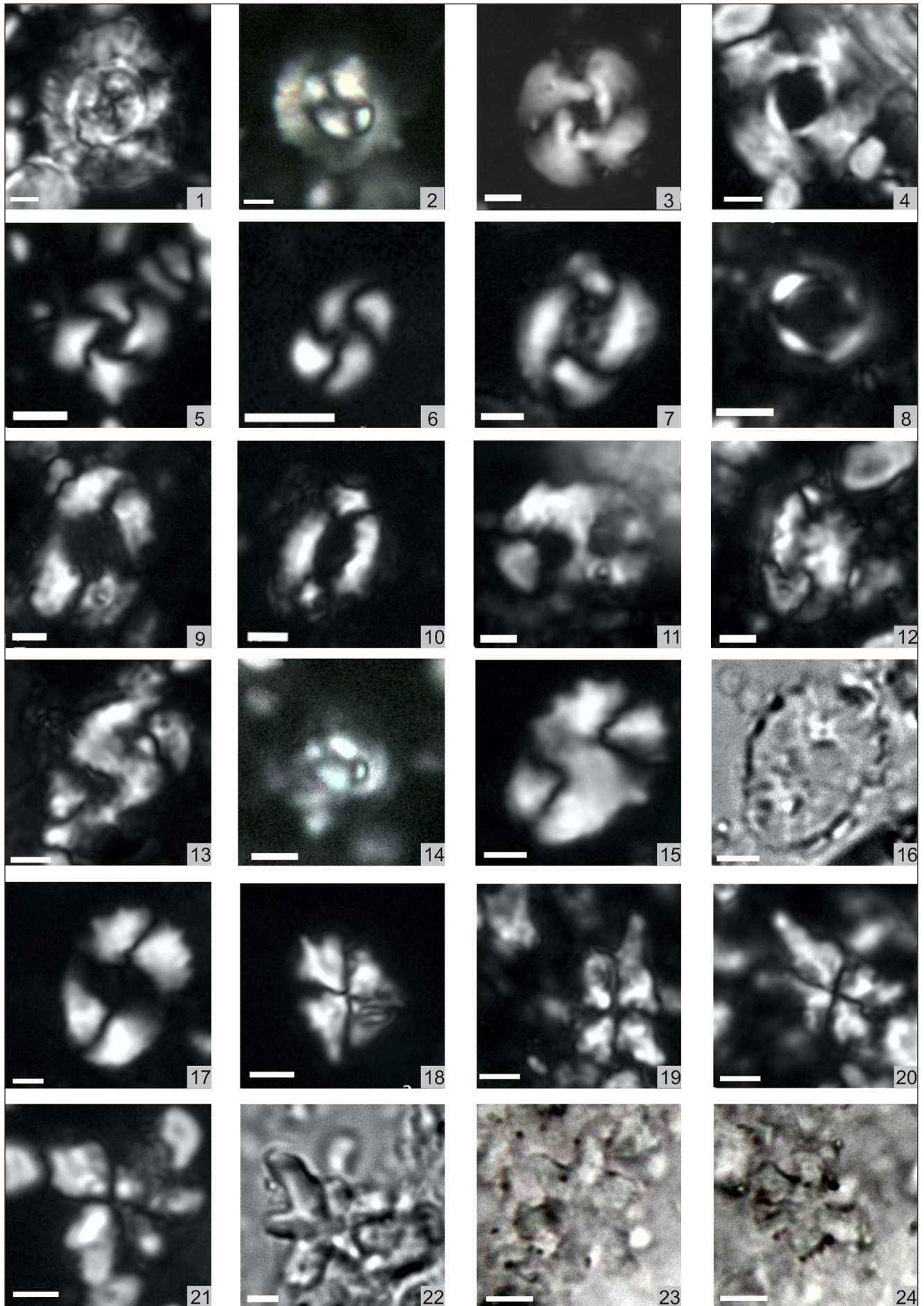


PLATE 2

The calcareous nannofossil assemblages identified in the sediments belonging to Qom Formation (Plate 2; Appendix 2), were assigned to the upper part of the long-ranging *Discoaster druggii* Zone (NN2; Martini 1971) and to *Discoaster druggii* Subzone of Okada and Bukry (Subzone CN1c; 1980), hence the studied sedimentary record is early Burdigalian. This study documents the co-occurrence of *Discoaster* cf. *druggii* (samples EQ23 and EQ53; Fig. 3; Plate 2, Figs. 22–24) which has its FO in the base of NN2 Zone (Young 1998) and that of *Helicosphaera ampliaperta* (samples EQ13 and EQ25; Fig. 3; Plate 2, Figs. 9–10) with a FO which approximates the Aquitanian/Burdigalian boundary (20.43 Ma; Gradstein et al. 2012). The updated new age for the FO of *H. ampliaperta* biohorizon in the Mediterranean area is 20.35 Ma (Fabbrini et al. 2019). The scarcity of *Sphenolithus pseudoheteromorphus* (samples EQ15 and EQ80; Fig. 3; Plate 2, Figs. 19–20) which has its FO in the upper part of NN2/CN1c zones (Fornaciari & Agnini 2009), support the age assignment of the studied sedimentary record, at least from sample EQ15 upward, to the lower Burdigalian (upper NN2 zone). This agrees with some observation made in the Mediterranean area (Albania), where lower Burdigalian assemblages with *H. ampliaperta* and *S. pseudoheteromorphus* were found (Kallanxhi 2023). The absence of *Sphenolithus belemnus* from the studied stratigraphic record, suggest that the studied sedimentary record is older than the FO of *S. belemnus* corresponding to the base of CN2/MNN3a/CNM5 zones (lower NN3 zone) and calibrated by Backman et al. (2012) to 19.01 Ma.

Other taxa used in Lower Miocene biostratigraphy are *Helicosphaera mediterranea* (samples EQ22, EQ23 and EQ24; Fig. 3; Plate 2, Fig. 11) and *Helicosphaera* cf. *watkinsii* (sample EQ19; Fig. 3; Plate 2, Fig. 13). *H. mediterranea* has its FO in the Mediterranean area within zones NN2/CN1c (DSDP Leg 42A, Hole 372; Müller 1981) and MNN2b subzone of Fornaciari & Rio (1996), above the FO of *H. ampliaperta*. This species occurs in the Lower Miocene from the middle – upper parts of zones NN2/CN1c in Albania, Mediterranean realm (Kallanxhi 2023). *Helicosphaera* cf. *watkinsii* (sample EQ19; Fig. 3; Plate 2, Fig. 13) is a short-ranging taxon restricted to Zone NN2 (da Gama & Varol 2013).

Other species with FO in Zone NN2 (Young

1998; Bergen et al. 2017; Boesiger et al. 2017) recovered from the studied sedimentary record are *R. haqii* (Fig. 3; Plate 2, Fig. 5), *U. rotula* (in samples EQ29 and EQ32), *H. vedderi* (sample EQ50), *S. dissimilis* (Fig. 3; Plate 2, Figs. 18, 21), which co-occurs with *R. pseudoumbilicus* (Fig. 3; Plate 2, Fig. 4). The specimens of this latter species are present in both sizes, but the larger morphotype ($>7\ \mu\text{m}$) is the dominant. Several authors (i.e., Fornaciari et al. 1996; Di Stefano et al. 2008) identify as *R. pseudoumbilicus* only the larger morphotypes, and suggest a younger FO (in NN6 Zone) for this species, compared to the FO at the base of NN4 Zone as in Nannotax3 (Young et al. 2022). The appearance of *R. pseudoumbilicus* ($>7\ \mu\text{m}$) within older sediments in Zone NN2 is however mentioned by some authors from the Atlantic Ocean (Howe & Sblendorio–Levy, 1998; Norris et al. 2014) and from the Central Paratethys (Molčíková & Straník 1987; Holcová 2013), whilst Kallanxhi (2023) reported recently both morphotypes of *R. pseudoumbilicus* starting with zone NN2 from the Mediterranean area.

Even though, the lower part of the section, from sample EQ1 to EQ13 (containing *Helicosphaera ampliaperta*) and EQ15 (containing *Sphenolithus pseudoheteromorphus*), lack the typical marker taxa, therefore it is not possible to constrain their age based on nannofossils.

Paleoenvironmental reconstruction

The most dominant morphotype throughout the section is the B1 with its most abundant genus *Ammonia*. This genus can be found in shallow brackish to hypersaline marine waters, generally living in a lagoon-like environment (Murray 1991, 2006), and it is the most common foraminiferal genus in shallow marine and paralic environments globally (Hayward et al. 2021). Therefore, we assign a shallow marine, relatively high energy depositional environment to the studied sedimentary record (Fig. 9). This is also supported by the taxa of the genera *Nonion*, *Elphidium*, and *Borelis*, which are mobile forms, and they can live and survive in the waters with high energy due to the shape of their test (Gonera 2012). The environment is further constrained by the *Elphidium*-taxa which often live in symbiosis with green algae, therefore their metabolism highly depends on photosynthesis and the depth of their habitat is controlled by the

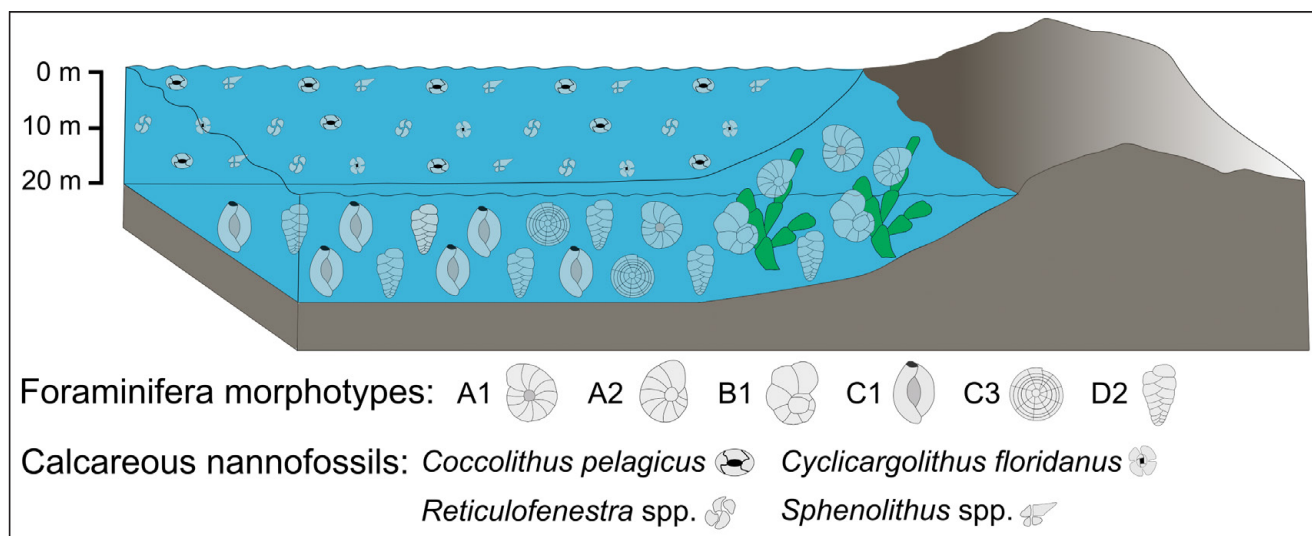


Fig. 9 - Paleoenvironmental reconstruction based on benthic foraminiferal assemblages. The figure also shows the distribution of benthic foraminiferal morphotypes.

symbiont's light demand (Leutenegger 1984). Although the *Textularia* and *Nodosaria* might suggest an even deeper environment (Parker & Gischler 2015), they are present in low abundance only. The very rare planktonic foraminifera recovered from some samples, are hard to be interpreted as it is not clear if they are in situ or not.

The environment was highly dynamic, as suggested by the 6 benthic foraminiferal groups (all of them of shallow marine origin) identified based on the hierarchical cluster and PCA-analysis. The dynamic changes of the paleoenvironment are however the best exemplified by the observed competition-like behavior noticed between *Ammonia beccarii* and *A. tepida* (Fig. 10): if one of them has a high relative abundance in a sample, the other species' relative abundance is low. In some samples however, their relative abundance is almost identical, but this is only observed when their relative abundance in a given sample is low. We explain this competition by environmental changes, as modern *A. beccarii* and *A. tepida* can present morphofunctional adaptations to their habitats and environment. *A. beccarii* can have an epiphytic mode of life thanks to a rapid 3-D emission of the pseudopodia, thus being able to support its test within the seaweed framework, whilst *A. tepida* has an inbenthic life mode, living in the sediment, and feeding on particulate organic matter (Debenay et al. 1998; Hayward et al. 2021). They also have dif-

ferent feeding strategies: laboratory experiments on the *A. beccarii* feeding habit showed that *A. beccarii* specimens might have a tendency of over-feeding to the point they consume and completely deplete the bacteria and algae supplies (Chandler 1989). Also, *A. beccarii* is known for its tolerance to different oxygen concentrations and it can survive even in a low-oxygen environment (Moodley & Hess 1992). Thus, when *A. beccarii* is the dominant then the paleoenvironment was either a well-oxygenated marine environment with seaweed or an environment with somewhat oxygen depleted bottom waters, whilst the dominance of *A. tepida* suggest a shallow-marine environment with higher sediment input, hence turbidity.

There is a high variation/fluctuation upwards the studied section until sample EQ-71 in the relative abundance of the high salinity tolerant species of C1 morphotype further suggesting dynamic changes and even salinity fluctuations within the shallow-marine paleoenvironment, as this change can be related to high evaporation rate, decrease or lack of freshwater input etc. (Murray 2006). Upwards from sample EQ-71 the relative abundance of C1 morphotype decreases, and it is replaced by the benthic foraminifera belonging to the B2 morphotype, known as high-energy species, surviving environments with fast-flowing waters, waves, and currents (Langer 1993). Thus, indicating a change in the ocean conditions.

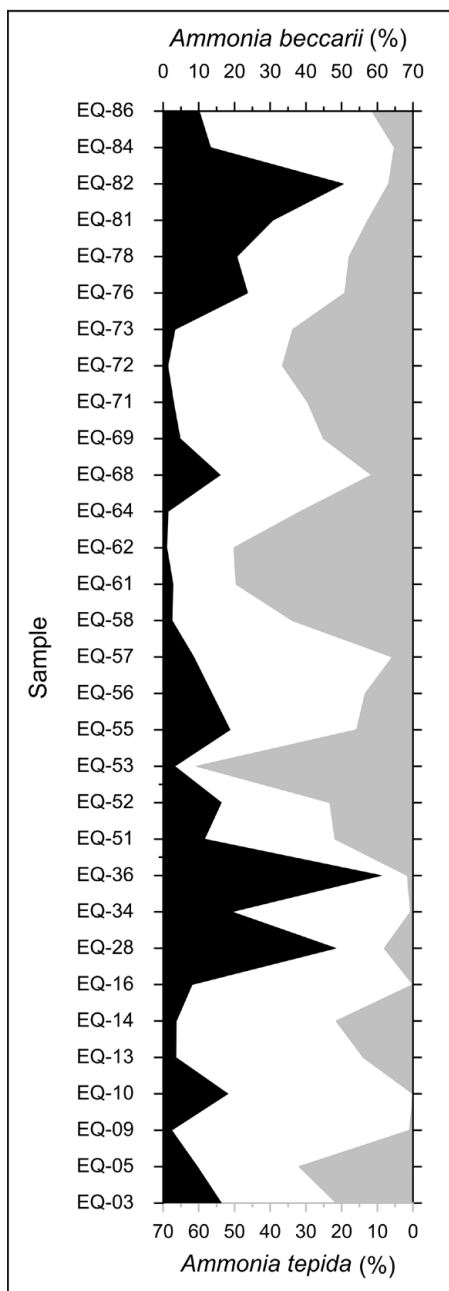


Fig. 10 - The relative abundance (%) of *Ammonia beccarii* (black) and *Ammonia tepida* (grey) along the studied section.

Paleoceanography

The birth of the Central Iranian Basin is linked to the collision and final subduction of the Arabian and African plates with the Iranian plate, which started in the Mesozoic (Coleman-Sadd 1982; Reuter et al. 2009; Rögl 1998a). As a result, during the Miocene, the so-called Tethyan Seaway was closed and consequently, the Qom Basin was formed (Reuter et al. 2009). In the Early Miocene a connection existed between the Paratethys, Mediterranean, and Indo-Pacific, which made pos-

sible in the early Burdigalian a substantial faunal migration between the Indo-Pacific and Paratethys (Harzhauser & Piller 2007; Rögl 1998a). However, this faunal migration and exchange between the Paratethys and the Indo-Pacific was terminated in the late Burdigalian because of the rotation and collision of the Arabian and African plates with Eurasia. This created the *Gomphotherium* Landbridge, thus connecting Africa with Eurasia (Rögl 1999). Al-Enezi et al. (2020) recently reported the genus *Olgita* from the coastal zone of Kuwait, the geographically closest, documented occurrence of this taxa to our sampling point. Therefore, our findings of the *O. pacifica* in the studied samples together with the existing palaeoceanographic data suggest the early Burdigalian age as a possible migration time of the species into the area of the Central Iranian Basin (Fig. 11).

CONCLUSIONS

Our study on the foraminiferal assemblages recovered from the Qom Formation offer new insights into its age and paleoenvironment. The recovered foraminiferal assemblages can be assigned to the *Borelis melo melo* Zone, hence the studied part of the Qom Formation was deposited during the Burdigalian (Early Miocene). This age assignment is further supported by the correlation to the upper part NN2 or CN1c calcareous nannofossil zones of the studied sedimentary record.

The benthic foraminiferal assemblages suggest a dynamic shallow-marine depositional environment, as emphasized by the abundance of the benthic foraminiferal species, and by the diversity of the benthic foraminiferal assemblages, and their clustering into six, well defined groups. These assemblages were controlled by the dynamic changes and even salinity fluctuations of the shallow-marine environment, and document a competition-like behavior between *Ammonia beccarii* and *Ammonia tepida*. The calcareous nannofossil assemblages recovered from the Qom Formation emphasize their potential in studies of shallow-marine sedimentary environments, and they proved to be useful to better constrain the time interval (early Burdigalian) when the connection through the Tethyan Seaway made possible the migration of *Olgita pacifica* into the Central Iranian Basin.

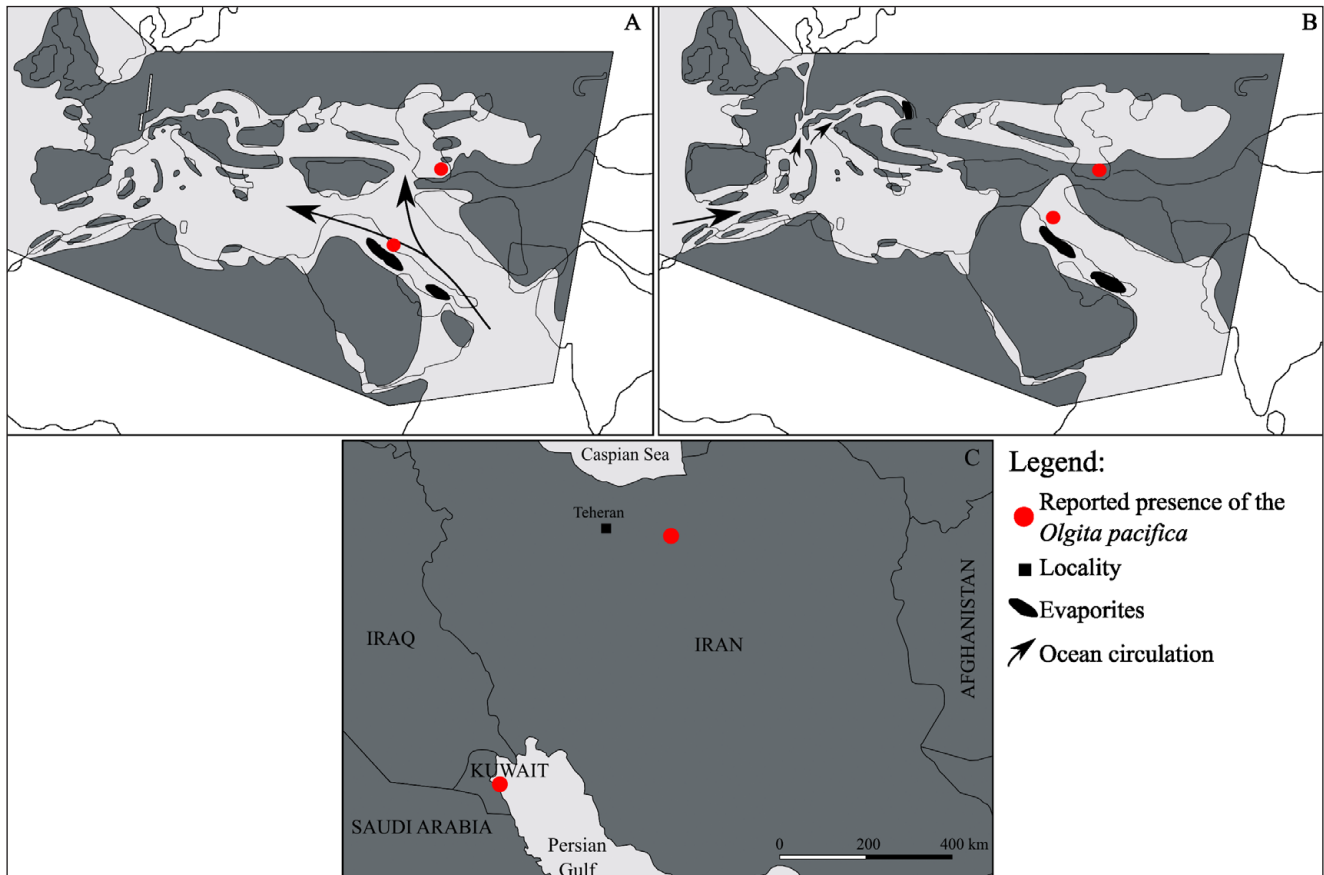


Fig. 11 - Simplified map of the spatial distribution of the foraminiferal genus *Olgita*. Reported presence and our findings. A: early Burdigalian paleogeography, B: late Burdigalian paleogeography, C: present-day geography (modified and redrawn after Rögl 1999).

Acknowledgements: This work was supported by the Collegium Talentum Program of Hungary. We thank Mike Kaminski (KFUPM) and an anonymous reviewer for their valuable comments and corrections to the manuscript.

REFERENCES

- Abaie I., Ansari H.J., Badakhshan A. & Jaafari A. (1964) - History and development of the Alborz and Sarajeh fields of Central Iran. *Bulletin of Iranian Petroleum Institute*, 15: 561-574.
- Abbassi N., Domning D.P., Navidi-Izad N. & Shakeri S. (2016) - Sirenia fossils from QOM formation (Burdigalian) of the Kabudar Ahang Area, Northwest Iran. *Rivista Italiana di Paleontologia e Stratigrafia*, 122(1): 13-24.
- Adams C.G., Gentry A.W. & Whybrow P.J. (1983) - Dating the terminal Tethyan event. *Utrecht Micropaleontology Bulletin*, 30: 273-298.
- Alavi-Naini M. (1997) - Geological map of Jam, scale 1:100000. Geol Survey of Iran.
- Al-Enezi E., Khader S., Balassi E. & Frontalini, F. (2020) - Modern Benthic Foraminiferal Diversity: An Initial Insight into the Total Foraminiferal Diversity along the Kuwait Coastal Water. *Diversity*, 12: no. 142.
- Backman J., Raffi I., Rio D., Fornaciari E. & Pälke H. (2012) - Biozonation and biochronology of Miocene through Pleistocene calcareous nannofossils from low and middle latitudes. *Newsletters on Stratigraphy*, 45: 221-244.
- Behforouzi E. & Safari A. (2011) - Biostratigraphy and paleoecology of the Qom Formation in Chenar area (north-western Khashan), Iran. *Revista Mexicana de Ciencias Geológicas*, 28(3): 555-556.
- Berberian M. (1983) - Continental deformation in the Iranian Plateau (Contribution to the seismotectonics of Iran, Part IV). Geological Survey of Iran, Report no. 52, 74 pp.
- Bergen J.A., de Kaenel E., Blair S.A., Boesiger T.M. & Browning E. (2017) - Oligocene Pliocene taxonomy and stratigraphy of the genus *Sphenolithus* in the circum North Atlantic Basin: Gulf of Mexico and ODP Leg 154. *Journal of Nannoplankton Research*, 37(2-3): 77-112.
- Betzler C. & Schmitz S. (1997) - First record of *Borelis melo* and *Dendritina* sp. in the Messinian of SE Spain (Cabo de Gata, Province Almeria). *Paläontologische Zeitschrift*, 71: 211-216.
- Boesiger T.M., de Kaenel E., Bergen J.A., Browning E. & Blair S.A. (2017) - Oligocene to Pleistocene taxonomy and stratigraphy of the genus *Helicosphaera* and other placolith taxa in the circum North Atlantic Basin. *Journal of Nannoplankton Research*, 37(2-3): 145-175.
- Bown P.R. & Young J.R. (1998) - Techniques. In: Bown P.R. (Ed.) - Calcareous nannofossil biostratigraphy: 16-28. Kluwer Academic Publications, Dordrecht.
- Bozorgnia F. (1966) - Qom formation stratigraphy of the Central Basin of Iran and its intercontinental position: *Bul-*

- letine of the Iranian Petroleum Institute, 24: 69-76.
- van Buchem F.S.P., Allan T.L., Laursen G.V. & Lotfpour M. (2010) - Regional stratigraphic architecture and reservoir types of the Oligo-Miocene deposits in the Dezful Embayment (Asmari and Pabdeh Formations) SW Iran. *Geological Society London Special Publications*, 329(1): 219-263.
- Chan S.A., Kaminski M.A., Al-Ramadan K. & Babalola L.O. (2017) - Foraminiferal biofacies and depositional environments of the Burdigalian mixed carbonate and siliciclastic Dam Formation, Al-Lidam area, Eastern Province of Saudi Arabia. *Palaeogeography, Palaeoclimatology, Palaeoecology*, 469: 122-137.
- Chandler G.T. (1989) - Foraminifera may structure meiobenthic communities. *Oecologia*, 81: 354-360.
- Coleman-Sadd S. (1982) - Two stage continental collision and plate driving forces. *Tectonophysics*, 90: 263-282.
- Corliss B.H. & Emerson S. (1990) - Distribution of Rose Bengal stained deep-sea benthic foraminifera from the Nova Scotian continental margin and Gulf of Maine. *Deep-Sea Research*, 37: 381-400.
- da Gama R.O.B.P. & Varol O. (2013) - New Late Oligocene to Miocene Species. *Journal of Nannoplankton Research*, 33(3): 1-12.
- Daneshian J. & Chegini A.R. (2007) - Biostratigraphy of the Qom Formation in the northeast and Southeast of Semnan. *Geosciences*, 16(62): 72-79.
- Daneshian J. & Dana L.R. (2007) - Early Miocene benthic foraminifera and biostratigraphy of the Qom Formation, Deh Namak, central Iran. *Journal of Asian Earth Sciences*, 29(5): 844-858.
- Daneshian J. & Dana L.R. (2019) - Benthic Foraminiferal Events of the Qom Formation in the North Central Iran Zone. *Paleontological Research* 23(1): 10-22.
- Daneshian J. & Ghanbari M. (2017) - Stratigraphic distribution of planktonic foraminifera from the Qom Formation: a case study from the Zanjan area (NW Central Iran). *Neues Jahrbuch für Geologie und Paläontologie - Abhandlungen*, 283(3): 239-254.
- Debenay J.-P., Bénéteau E., Zhang J., Stouff V., Geslin E., Redois F. & Fernandez-Gonzalez M. (1998) - *Ammonia beccarii* and *Ammonia tepida* (Foraminifera): morphofunctional arguments for their distinction. *Marine Micropaleontology*, 34: 235-244.
- Di Stefano A., Foresi L.M., Lirer F., Iaccarino S.M., Turco E., Amore F.O., Mazzei R., Morabito S., Salvatorini G. & Abdul Aziz H. (2008) - Calcareous plankton high resolution bio-magnetostratigraphy for the Langhian of the Mediterranean area. *Rivista Italiana di Paleontologia e Stratigrafia*, 114(1): 51-76.
- El Baz S.M. & Al Furjany A. (2018) - Middle Miocene benthic foraminifera from the Al Khums area, northwestern Libya. *Journal of African Earth Sciences*, 138: 112-123.
- Fabbrini A., Baldassini N., Caricchi C., Foresi L.M., Sagnotti L., Dinarès-Turell J., Di Stefano A., Lirer F., Menichetti M., Winkler A. & Distefano S. (2019) - In search of the Burdigalian GSSP: new evidence from the Contessa Section (Italy). *Italian Journal of Geosciences*, 138: 274-295.
- Fisher R.A., Corbet A.S. & Williams C.B. (1943) - The relation between the number of species and the number of individuals in a random sample of an animal population. *Journal of Animal Ecology*, 12: 42-58.
- Fornaciari E. & Agnini C. (2009) - Taxonomic note: *Sphenolithus pseudoheteromorphus*, a new Miocene calcareous nannofossil species from the equatorial Indian Ocean. *Journal of Nannoplankton Research*, 30(2): 97-101.
- Fornaciari E. & Rio D. (1996) - Latest Oligocene to early middle Miocene quantitative calcareous nannofossil biostratigraphy in the Mediterranean region. *Micropaleontology*, 42(1): 1-36.
- Fornaciari E., Di Stefano A., Rio D. & Negri A. (1996) - Middle Miocene quantitative calcareous nannofossil biostratigraphy in the Mediterranean region. *Micropaleontology*, 42(1): 37-63.
- Frezza V. & Carboni M.G. (2009) - Distribution of recent foraminiferal assemblages near the Ombrone River mouth (Northern Tyrrhenian Sea, Italy). *Revue de Micropaléontologie*, 52(1): 43-66.
- Furrer M.A. & Sonder P.A. (1955) - The Oligo-Miocene Formation in the Qom region (Iran). *Proceedings of the 4th World Petroleum Congress, Rome, Section I/A/5*: 267-277.
- Gansser A. (1955) - New aspects of the geology in Central Iran. *Proceedings of the 4th World Petroleum Congress, Rome, Section I/A/5*: 279-300.
- Gonera M. (2012) - Palaeoecology of the Middle Miocene foraminifera of the Nowy Sącz Basin (Polish Outer Carpathians). *Geological Quarterly*, 56(1): 107-116.
- Gradstein F.M., Ogg J.G., Schmitz M.D. & Ogg G.M. (Eds.) (2012) - The Geologic Time Scale 2012, *Elsevier*, Amsterdam, 1-1144.
- Hammer Ø. & Harper D.A.T. (2006) - Paleontological Data Analysis. Oxford, Blackwell, 351 pp.
- Hammer Ø., Harper D.A.T. & Ryan P.D. (2001) - PAST: Paleontological Statistics Software Package for Education and Data Analysis. *Palaeontologia Electronica*, 4(1): art 4.
- Harzhauser M. & Piller W.E. (2007) - Benchmark data of a changing sea: palaeogeography, palaeobiogeography and events in the Central Paratethys during the Miocene. *Palaeogeography, Palaeoclimatology, Palaeoecology*, 253(1-4): 8-31.
- Haunold T.G. (1999) - Ecologically controlled distribution of recent Textulariid foraminifera in subtropical, carbonate-rich Safaga Bay (Red Sea, Egypt). *Beiträge zur Paläontologie*, 24: 69-85.
- Heidari A., Mahboubi A., Moussavi-Harami R., Gonzalez L. & Moalemi S.A. (2014) - Biostratigraphy, sequence stratigraphy, and paleoecology of the Lower-Middle Miocene of Northern Bandar Abbas, Southeast Zagros basin in south of Iran. *Arabian Journal of Geosciences*, 7(5): 1829-1855.
- Hayward B. W., Holzmann M., Pawlowski J., Parker J. H., Kaushik T., Toyofuku M. S. & Tsuchiya M. (2021) - Molecular and morphological taxonomy of living *Ammonia* and related taxa (Foraminifera) and their biogeography. *Micropaleontology*, 67(2-3): 109-313.
- Hermelin J.O. & Shimmield G.B. (1990) - The importance of the oxygen minimum zone and sediment geochemistry in the distribution of Recent benthic foraminifera in the northwest Indian Ocean. *Marine Geology*, 91: 1-29.
- Heydari E., Hassanzadeh J., Wade W.J. & Ghazi A.M. (2003) - Permian-Triassic boundary interval in the Abadeh section of Iran with implications for mass extinction: Part 1-Sedimentology. *Palaeogeography, Palaeoclimatology, Palaeoecology*, 193(3-4): 405-423.
- Hilgen F.J., Lourens L.J., Van Dam J.A., Beu A.G., Boyes A.F., Cooper R.A., Krijgsman W., Ogg J.G., Piller W.E. & Wilson D.S. (2012). Chapter 29 - The Neogene Period. In: Gradstein F.M., Ogg J.G., Schmitz M.D. & Ogg G.M. (Eds.) - The Geologic Time Scale: 923-978. Elsevier, Boston.

- Holcová K. (2013) - Morphological variability of the Paratethyan Oligocene–Miocene small reticulofenestrid coccolites and its paleoecological and paleogeographical implications. *Acta Palaeontologica Polonica*, 58(3): 651–668.
- Howe R.W. & Sblendorio-Levy J. (1998) - Calcareous nanofossil biostratigraphy and sediment accumulation of turbidite sequences on the Madeira Abyssal Plain, ODP Sites 950 – 952. *Proc. Ocean Drill. Proj. Sci. Results*, 157: 501–520.
- Hughes G.W. (2014) - Micropalaeontology and palaeoenvironments of the Miocene Wadi Waqb carbonate of the northern Saudi Arabian Red Sea. *GeoArabia*, 19(4): 59–108.
- Kallanxhi M.-E. (2023) - Biostratigraphy of calcareous nanofossils and palaeoenvironments in the Lower Miocene of the Albanian–Thessalian Basin (Albania). *Geologica Carpathica*, 74(1): 41–58.
- Karevan M., Vaziri-Moghaddam H., Mahboubi A. & Moussavi-Harami R. (2014) - Biostratigraphy and paleo-ecological reconstruction on Scleractinian reef corals of Rupelian–Chattian succession (Qom Formation) in northeast of Delijan area. *Geopersia*, 4: 11–24.
- Kitazato H. & Tsuchiya M. (1999) - Why are foraminifera useful proxies for modern and ancient marine environments? An example using *Ammonia beccarii* (Linné) from brackish inner bay environments. *Kagoshima University Research Center for the Pacific Islands Occasional Papers*, 32: 3–17.
- Kühn O. (1933) - Das Becken von Isfahan-Saidabad und seine altmiocene Korallenfauna. *Palaeontographica*, 79: 143–221.
- Langer R.M. (1993) - Epiphytic foraminifera. *Marine Micropaleontology*, 20(3–4): 235–265.
- Laursen G.V., Monibi S., Allan T.L., Pickard N.A.H., Hosseiny A., Vincent B., Hamon Y., van Buchem F.S.P., Moallemi A. & Druillion G. (2009) - The Asmari Formation Revisited: Changed Stratigraphic Allocation and New Biozonation. First International Petroleum Conference & Exhibition Shiraz, Iran, B29 :1–5.
- Letouzey J. & Rudkiewicz J. (2005) - Structural geology in the Central Iranian Basin. Institut Français du Pétrole report F0214001, 79 pp.
- Leutenegger S. (1984) - Symbiosis in benthic foraminifera; specificity and host adaptations. *Journal of Foraminiferal Research*, 14(1): 16–35.
- Levy A., Mathieu R., Poignant A., Rosset-Moulinier Ubaldo M.L. & Lebreiro S. (1995) - Foraminifères actuels de la Marge Continentale Portugaise-Inventaire et distribution. *Memórias do Instituto Geológico e Mineiro*, 32: 3–116.
- Loftus W.K. (1855) - On the geology of the Turko-Persian Frontier and of the districts adjoining, Quart. *Journal of Geological Society of London*, 11: 247–344.
- Martini E. (1971) - Standard Tertiary and Quaternary calcareous nannoplankton zonations. In: Farinacci A. (Ed.) - Proceedings 2nd International Conference on Planktonic Microfossils, Roma 1970. *Edizioni Tecnoscienza*, Roma, 2: 739–785.
- Mendes I., Gonzalez R., Dias J.M.A., Lobo F. & Martins V. (2004) - Factors influencing recent benthic foraminifera distribution on the Guadiana shelf (Southwestern Iberia). *Marine Micropaleontology*, 51(1–2): 171–192.
- Miller K.G. & Lohmann G.P. (1982) - Environmental distribution of recent benthic foraminifera of the northeast United States continental slope. *Geological Society of America Bulletin*, 93: 200–206.
- Mohammadi E. & Ameri H. (2015) - Biotic components and biostratigraphy of the Qom Formation in northern Abadeh, Sanandaj–Sirjan fore-arc basin, Iran (northeastern margin of the Tethyan Seaway). *Arabian Journal of Geosciences*, 8: 10789–10802.
- Mohammadi E. (2022) - Foraminiferal biozonation, biostratigraphy and trans-basinal correlation of the Oligo-Miocene Qom Formation, Iran (northeastern margin of the Tethyan Seaway). *Palaeoworld*, 32(1): 156–173.
- Mohammadi E., Hasanzadeh-Dastgerdi M., Ghaedi M., Dehghan R., Safari A., Vaziri-Moghaddam H., Baizidi C., Vaziri M. & Sfidari E. (2013) - The Tethyan Seaway Iranian Plate Oligo-Miocene deposits (the Qom Formation): distribution of Rupelian (Early Oligocene) and evaporate deposits as evidences for timing and trending of opening and closure of the Tethyan Seaway. *Carbonates and Evaporites*, 28: 321–345.
- Molčíková V. & Straník Z. (1987) - Vápňitý nanoplankton ze ždánicko-hustopečského souvrství a jeho vztah k nadloží. *Knibovníčka ZPN*, 6B(2/2): 59–76.
- Moodley L. & Hess C. (1992) - Tolerance of Infaunal Benthic Foraminifera for Low and High Oxygen Concentrations. *The Biological Bulletin*, 183(1): 94–98.
- Morigi C., Jorissen F.J., Fraticelli S., Horton B.P., Principi M., Sabbatini A., Capotondi L., Curzi P.V. & Negri A. (2005) - Benthic foraminiferal evidence for the formation of the Holocene mud-belt and bathymetrical evolution in the central Adriatic Sea. *Marine Micropaleontology*, 57(1–2): 25–49.
- Murray J.W. (1991) - Ecology and Palaeoecology of Benthic Foraminifera. Longman Scientific & Technical, Harlow, 397 pp.
- Murray J.W. (2006) - Ecology and Applications of Benthic Foraminifera. Cambridge University Press, Cambridge, 426 pp.
- Müller C. (1981) - Description of new *Helicosphaera* species from the Miocene and revision of the biostratigraphic ranges of some Neogene nannoplankton species. *Senckenbergiana Lethaea*, 61: 427–435 (in German).
- Norris R.D., Wilson P.A., Blum P., Fehr A., Agnini C., Bornemann A., Boulila S., Bown P.R., Cournede C., Friedrich O., Ghosh A.K., Hollis C.J., Hull P.M., Jo K., Junium C.K., Kaneko M., Liebrand D., Lippert P.C., Liu Z., Matsui H., Moriya K., Nishi H., Opdyke B.N., Penman D., Romans B., Scher H.D., Sexton P., Takagi H., Turner S.K., Whiteside J.H., Yamaguchi T. & Yamamoto Y. (2014) - Site U1406. In Norris R.D., Wilson P.A., Blum P., and the Expedition 342 Scientists, Proc. IODP, 342: College Station, TX (Integrated Ocean Drilling Program).
- Nouradini M., Azami S.H., Hamad M., Yazdi M. & Ashouri A.R. (2015) - Foraminiferal paleoecology and paleoenvironmental reconstructions of the lower Miocene deposits of the Qom Formation in Northeastern Isfahan Central Iran. *Boletín de la Sociedad Geológica Mexicana*, 67(1): 59–73.
- Okada H. & Bukry D. (1980) - Supplementary modification and introduction of code numbers to the low-latitude coccolith biostratigraphic zonation (Bukry, 1973; 1975). *Marine Micropaleontology*, 5: 321–325.
- Parker J.H. & Gischler E. (2015) - Modern and relict foraminiferal biofacies from a carbonate ramp, offshore Kuwait, northwest Persian Gulf. *Facies*, 61: art. 10, <https://doi.org/10.1007/s10347-015-0437-5>.
- Polvodova I., Nikulina A., Schönfeld J. & Dullo W.-C. (2009)

- Recent benthic foraminifera in the Flensburg Fjord (Western Baltic Sea). *Journal of Micropalaeontology*, 28(2): 131-142.
- Rahaghi A. (1976) - Contribution à l'étude de quelques grands foraminifères de l'Iran Parts 1-3. Société Nationale Iranienne des Pétroles, Laboratoire de Micropaléontologie, Tehran, 79 pp.
- Rahaghi A. (1980) - Tertiary faunal assemblage of Qum-Kashan, Sabzewar and Jahrum areas. Ministry of Oil, National Iranian Oil Co., Geological Laboratories, Tehran, 64 pp.
- Reiss Z. & Hottinger L. (1984) - The Gulf of Aqaba: Ecological micropaleontology. Springer Verlag, Berlin, 354 pp.
- Reuter M., Pillar W.E., Harzhauser M., Mandic O., Berning B., Rögl F., Kroh A., Aubry M.P., Wielandt-Schuster U. & Hamedani A. (2009) - The Oligo-Miocene Qom Formation (Iran): evidence for an early Burdigalian restriction of Tethyan Seaway and clouser of its Iranian gateways. *International Journal of Earth Sciences*, 98: 627-650.
- Rezaeian M. (2008) - Coupled tectonics, erosion and climate in the Alborz Mountains, Iran. PhD thesis, University of Cambridge, Cambridge, 219 pp.
- Robba E. (1986) - The final occlusion of Tethys: its bearing on Mediterranean benthic molluscs. *Proceedings of the International Symposium on Shallow Tethys*, 2: 405-426.
- Rögl F. & Steininger F.F. (1983) - Vom Zerfall der Tethys zu Mediterran und Paratethys. Die neogene Paläogeographie und Palinspastik des zirkum-mediterranen Baumes. *Annalen des Naturhistorischen Museums in Wien, Serie A*, 85: 135-163.
- Rögl F. (1998a) - Palaeogeographic Considerations for Mediterranean and Paratethys Seaways (Oligocene and Miocene). *Annalen des Naturhistorischen Museums in Wien*, 99A: 279-310.
- Rögl F. (1998b) - Paratethys Oligocene-Miocene stratigraphic correlation. In: Cicha I., Rögl F., Rupp C. & Ctyroka J. (Eds.) - Oligocene - Miocene foraminifera of the Central Paratethys, *Abhandlungen der Senckenbergischen Naturforschenden Gesellschaft*, 549: 3-7.
- Rögl F. (1999) - Mediterranean and Paratethys. Facts and hypotheses of an Oligocene to Miocene Paleogeography (short overview). *Geologica Carpathica*, 50(4): 339-349.
- Sakhavati B., Yousefirad M., Majidifard M.R., Solgi A. & Maleki Z. (2020) - Age of the Gachsaran Formation and equivalent formations in the Middle East based on Foraminifera. *Micropaleontology*, 66(5): 441-465.
- Schuster F. & Wielandt U. (1999) - Oligocene and Early Miocene coral faunas from Iran: palaeoecology and palaeobiogeography. *International Journal of Earth Sciences*, 3: 571-581.
- Seddighi M., Vaziri-Moghaddam H., Taheri A. & Ghabeishavi A. (2012) - Depositional environment and constraining factors on the facies architecture of the Qom Formation, Central Basin, Iran. *Historical Biology*, 24: 91-100.
- Seyrafian A. & Toraby H. (2005) - Petrofacies and sequence stratigraphy of the Qom Formation (Late Oligocene-Early Miocene?), north of Nain, southern trend of central Iranian Basin. *Carbonates and Evaporites*, 20: 82-90.
- Soder P.A. (1959) - Detailed investigations on the marine Formation of Qum, 2nd report. National Iranian Oil Company Geological Report no. 185, 58 pp.
- Spellerberg I.F. & Fedor P.J. (2003) - A tribute to Claude Shannon (1916–2001) and a plea for more rigorous use of species richness, species diversity and the “Shannon–Wiener” index. *Global Ecology and Biogeography*, 12(3): 177-179.
- Stöcklin J. & Setudehina A. (1991) - Stratigraphic lexicon of Iran. Geological Survey of Iran, Report 18, p. 1-376.
- The Geological Staff of the Iran Oil Company (1957). Geological Map of Iran, 1:2.500.000, National Oil Company of Iran.
- Tietze E. (1875) - Ein Ausflug nach dem Siaskuh (Schwarzer Berg) in Persien. *Mitteilung Geographische Gesellschaft*, 18(8): 257-267.
- Vaziri-Moghaddam H., Seyrafian A., Taheri A. & Motiei H. (2010) - Oligocene-Miocene ramp system (Asmari Formation) in the NW of the Zagros basin, Iran: microfacies, paleoenvironment and depositional sequence. *Revista Mexicana de Ciencias Geológicas*, 27(1): 56-71.
- Wade B.S. & Bown P.R. (2006) - Calcareous nannofossils in extreme environments: The Messinian Salinity Crisis. Polemi Basin, Cyprus. *Palaeogeography Palaeoclimatology Palaeoecology* 233(3-4): 271-286.
- Whybrow P.J. (1984) - Geological and faunal evidence from Arabia formammal migrations between Asia and Africa during the Miocene. *Courier Forschungsinstitut Senckenberg*, 69: 189-198.
- Yazdi-Moghaddam M., Sadeghi A., Adabi M.H. & Tahmasbi A. (2018) - Foraminiferal biostratigraphy of the lower Miocene Hamzian and Arashtanab sections (NW Iran), northern margin of the Tethyan Seaway. *Geobios*, 51(3): 231-246.
- Yazdi-Moghaddam M., Sarfi M., Ghasemi-Nejad E., Sadeghi A. & Sharifi M. (2021) - Early Miocene larger benthic foraminifera from the northwestern Tethyan Seaway (NW Iran): new findings on Shallow Benthic Zone 25. *International Journal of Earth Sciences*, 110: 719-740.
- Young J.R. (1998) - Neogene. In: Bown P.R. (Ed.) - Calcareous nannofossil biostratigraphy. *Kluwer Academic Publications, Dordrecht*, 225-265.
- Young J.R., Bown P.R. & Lees J.A. (2022) - Nannotax3 website. International Nannoplankton Association. Accessed 11 May 2023. URL: www.mikrotax.org/Nannotax3